Recent Advances in the Theory of Lagrangian Coherent Structures for Three-Dimensional Flows

David Oettinger* and George Haller*
Institute for Mechanical Systems, ETH Zürich, Leonhardstrasse 21, 8092 Zürich, Switzerland

Summary. Lagrangian coherent structures (LCSs) are generalizations of classical invariant manifolds to time-aperiodic dynamical systems defined over finite time intervals. Computing LCSs in three dimensional systems, however, remains challenging. Here we present details of our numerical techniques and discuss several applications, in particular the dynamics of inertial particles in fluid flows.

Introduction

Fluid flows observed in nature, experiments or numerical simulations often produce visually striking tracer patterns (cf. Fig. 1). The ubiquity of these patterns even in complicated time-aperiodic flows suggests the existence of influential and robust manifolds that create coherence in the configuration space of fluid particle positions. These manifolds act as observable barriers to transport and have been termed *Lagrangian coherent structures* (LCSs) [1]. In the classic setting of autonomous or time-periodic dynamical systems, similar transport barriers are, e.g., Komolgorov-Arnold-Moser tori.

Figure 1: (a) Sea surface temperature in the Gulf Stream (Image: NASA), (b) tornado near Anadarko, Oklahoma (Image: NOAA), (c) coherent vortex ring (blue) exerting exceptional impact on nearby tracer particles (red) (Image: David Oettinger).

Mathematical Setting: Finite-time Dynamical Systems

Since fluid velocity fields obtained from measurements and numerical computations are only available for finite time intervals, we consider the finite-time dynamical system

$$\dot{\boldsymbol{x}} = \boldsymbol{v}(\boldsymbol{x}, t), \quad \boldsymbol{x} \in U, \quad t \in [t_0, t_1], \tag{1}$$

where $\boldsymbol{v}$ is a smooth three-dimensional vector field on an open set $U \subset \mathbb{R}^3$ with arbitrary smooth dependence on time t; t_0, t_1 are initial and final times. For any two times $t_a, t_b \in [t_0, t_1]$, trajectories of (1) define the flow map $\boldsymbol{F}_{t_a}^{t_b} : \boldsymbol{x}_a \mapsto \boldsymbol{x}_b$ that uniquely maps the time-t_a position $\boldsymbol{x}_a$ of any particle to its time-t_b position $\boldsymbol{x}_b$ (cf. Fig. 2(a)). By a *particle* we mean either a fluid particle following precisely the surrounding fluid velocity field $\boldsymbol{u}$, i.e., $\boldsymbol{v} = \boldsymbol{u}$, or an inertial particle following a vector field $\boldsymbol{v}$ that deviates from $\boldsymbol{u}$. We note that even though many concepts we present here are motivated by applications to fluid dynamics, they remain well-defined for any differentiable dynamical system.

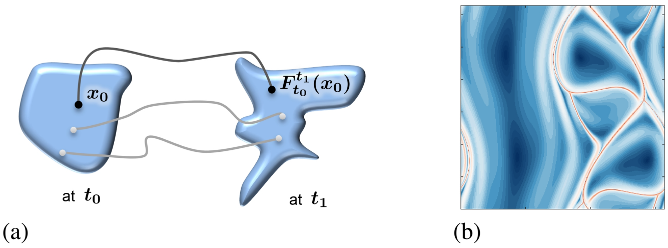

Figure 2: (a) Flow map $\boldsymbol{F}_{t_0}^{t_1}$ mapping initial material positions at time t_0 to their final positions at t_1, with the gray lines indicating trajectories of (1). (Image: David Oettinger) (b) FTLE visualization of an ABC flow, with low FTLE values (blue) highlighting vortical regions, and high FTLE values (red) highlighting hyperbolic structures. (Image: David Oettinger)

The derivative $\boldsymbol{DF}_{t_0}^{t_1}(\boldsymbol{x}_0)$ of the flow map at any time-t_0 position $\boldsymbol{x}_0$ is known as the deformation gradient. We can view $\boldsymbol{DF}_{t_0}^{t_1}(\boldsymbol{x}_0)$ as a three-by-three matrix containing local information on how the fluid stretches and shrinks between times t_0 and t_1. In particular, the largest singular value of $\boldsymbol{DF}_{t_0}^{t_1}(\boldsymbol{x}_0)$ is the *finite-time Lyapunov exponent* (FTLE, see, e.g. [1]), highlighting locations of exceptional separation in the fluid flow. In applications, FTLE fields have become a widely-popular diagnostic for generalized stable and unstable manifolds (repelling and attracting hyperbolic LCSs, cf. Fig. 2(b)).

LCSs in Three Dimensions and Computational Challenges

In recent years, well-documented shortcomings of using FTLE features to define LCSs have led to the development of variational LCS theories [1]. In three dimensions, variational definitions of hyperbolic and elliptic LCSs (generalized invariant tori and cylinders) are available [2, 3]. Recently, we have observed that all LCSs in three dimensions are two-dimensional invariant manifolds of an autonomous dynamical system defined on the flow domain at the fixed time t_0 (cf. [4] and Fig. 3). Specifically, this autonomous system is given by

$$\boldsymbol{x}_0' = \boldsymbol{\xi}_2(\boldsymbol{x}_0), \tag{2}$$

where $\boldsymbol{x}_0$ denotes time-t_0 positions, and $\boldsymbol{\xi}_2(\boldsymbol{x}_0)$ is the intermediate right-singular vector of the deformation gradient $\boldsymbol{DF}_{t_0}^{t_1}(\boldsymbol{x}_0)$. Here we address technical challenges that arise in the computation of LCSs for finite-time systems (1)

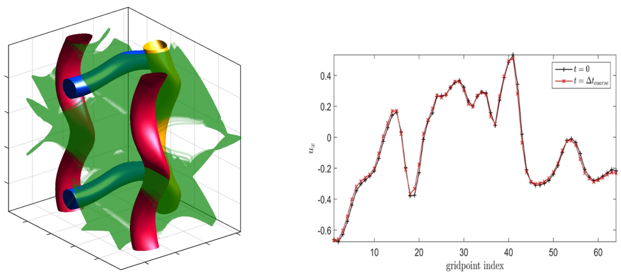

(a) (b)

Figure 3: (a) Hyperbolic and elliptic LCSs in a time-aperiodic ABC-type flow [4] (b) Consecutive snapshots of a velocity field component in forced isotropic turbulence (Image: David Oettinger, with data obtained from the JHTDB at *http://turbulence.pha.jhu.edu*)

given by numerical data (cf. Fig. 3 (b)): in particular, the interpolation of the velocity field, grid resolution, numerical preservation of incompressibility, and discretization of the domain of initial positions $\boldsymbol{x}_0$.

Accumulation of Inertial Particles

Another direction of new developments is understanding the dynamics of inertial particles in three-dimensional unsteady flows (small bubbles or heavy particles). To leading order, these obey the inertial equation

$$\dot{\boldsymbol{x}} = \boldsymbol{v}(\boldsymbol{x}, t) = \boldsymbol{u}(\boldsymbol{x}, t) + \varepsilon \boldsymbol{D}_{\boldsymbol{x}} \boldsymbol{u}(\boldsymbol{x}, t), \tag{3}$$

where $\boldsymbol{u}$ is the fluid velocity field and $\varepsilon > 0$ is a small parameter [5]. Even for incompressible fluids, the system (3) is generally dissipative, i.e., $\boldsymbol{\nabla} \cdot \boldsymbol{v} \neq 0$. Inertial particles are hence expected to accumulate on attractors. For the general setting of three-dimensional unsteady flows (1), however, no generally-accepted method for identifying all the attractors of (3) has emerged. Here we apply our techniques for three-dimensional LCSs and compute transport barriers for inertial particles in practically relevant applications (cf. Fig. 4).

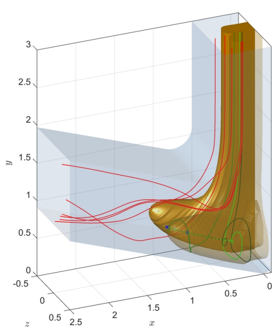

Figure 4: Invariant manifolds (yellow) causing the capture of gas bubbles in a hydrodynamic flow through a V Junction, together with representative bubble trajectories (green and red). (Image: David Oettinger, from joint work with Jesse T. Ault and Howard A. Stone)

References

[1] G. Haller. Lagrangian Coherent Structures. *Annual Review of Fluid Mechanics*, 47(1):137–162, 2015.

[2] D. Blazevski and G. Haller. Hyperbolic and elliptic transport barriers in three-dimensional unsteady flows. *Physica D*, 273-274:46 – 62, 2014.

[3] D. Oettinger, D. Blazevski, and G. Haller. Global variational approach to elliptic transport barriers in three dimensions. *Chaos*, 26(3):033114, 2016.

[4] D. Oettinger and G. Haller. An autonomous dynamical system captures all LCSs in three-dimensional unsteady flows. *Chaos*, 26(10):103111, 2016.

[5] G. Haller and T. Sapsis. Where do inertial particles go in fluid flows? *Physica D*, 237:573 – 583, 2008.